Estimation of ripple and inductance roll off when using powdered iron core inductors

Chandra Mouli, Gautham Ram; Schijffelen, Jos; Bauer, Pavol; Zeman, Miro

Publication date
2016

Document Version
Accepted author manuscript

Published in
Proceedings of PCIM Europe 2016 International Exhibition and Conference for Power Electronics, Intelligent Motion, Renewable Energy and Energy Management

Citation (APA)
Chandra Mouli, G. R., Schijffelen, J., Bauer, P., & Zeman, M. (2016). Estimation of ripple and inductance roll off when using powdered iron core inductors. In *Proceedings of PCIM Europe 2016 International Exhibition and Conference for Power Electronics, Intelligent Motion, Renewable Energy and Energy Management* (pp. 1383-1390). VDE Verlag GMBH. http://ieeexplore.ieee.org/document/7499515/?arnumber=7499515

Estimation of ripple and inductance roll off when using powdered iron core inductors

Gautham Ram Chandra Mouli[1], Jos Schijffelen[2], Pavol Bauer[1], Miro Zeman[1]
[1]Department of Electrical Sustainable Energy, Delft University of Technology, Netherlands (G.R.Chandramouli@tudelft.nl, P.Bauer@tudelft.nl, M.Zeman@tudelft.nl)
[2]Power Research Electronics BV, Netherlands (j.schijffelen@pr-electronics.nl)

Abstract

Magnetic cores like powdered iron cores have a variable permeability, which is dependent on the magnetic motive force of the inductor windings. When inductors are designed using such materials, the inductance varies as a function of the inductor current. This causes a non-linear current to flow through the inductor. In this paper, mathematical derivation of the inductance-current relationship is derived for such inductors. The model is applied for a KoolMμ® powdered iron core and the results are verified experimentally using an interleaved boost converter.

1. Introduction

Inductors are widely used in DC/DC converters as an energy storage element and as a filter. The inductance *L* can be related to the number of turns of the copper wire *N*, core material and the dimensions of the core by

$$L = \left(\frac{\mu_0 \mu_r A_c}{l_e}\right) N^2 = A_L N^2 \qquad where \quad A_L = \left(\frac{\mu_0 \mu_r A_c}{l_e}\right) \tag{1}$$

where μ_0=4πx10^{-7}, μ_r - relative permeability of the material, A_c - core area, l_e - magnetic path length, A_L is permeance of the material.

When a DC voltage V_L is applied across the inductor, the current through the inductor i_L linearly increases/decreases based on the sign of the voltage where $i_{L(0)}$ is the inductor current at time *t=0*, Δi_L is the current ripple in time Δt:

$$V_L = L\frac{di_L}{dt} \qquad \Delta i_L = i_L(t) - i_{L(0)} = \frac{V_L}{L}\Delta t \tag{2}$$

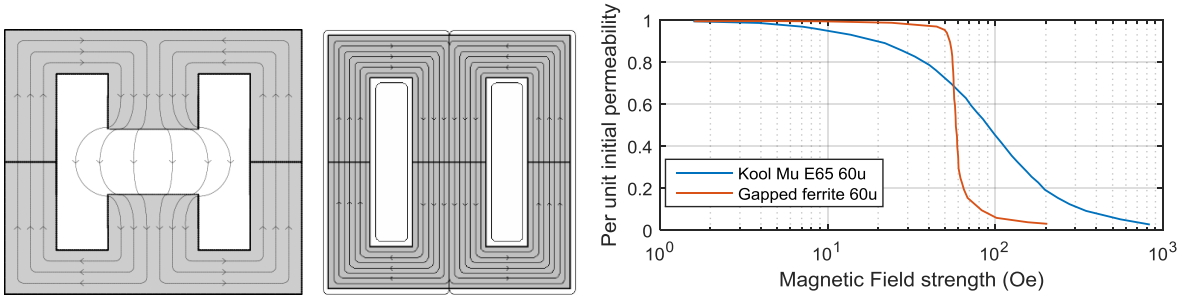

Fig. 1. Path of flux lines through a gapped ferrite core (left) and a powdered iron core (middle). Variation of permeability of core as a function of magnetic field strength for a KoolMμ powdered iron core and gapped ferrite core, both of which have an initial permeability of μ_r=60 (right) [1]

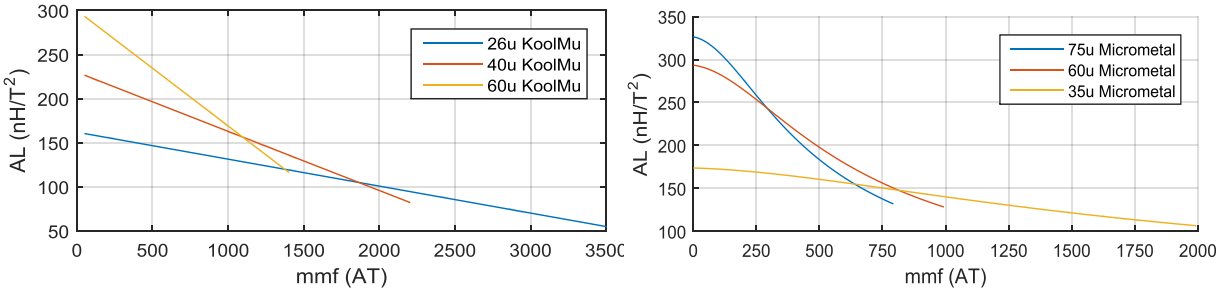

Fig. 2. Permeance A_L of three core of different permeability as a function of the ampere-turns for KoolMμ E65 (left) and Micrometal E-255 (right). The permeance and inductance of the core reduces linearly with increase in current through the inductor.

When inductors are designed using ferrite cores, the core exhibits a practically constant permeability and permeance in the operating region. This is because it has a fixed air gap and the reluctance of the core is primarily characterized by this air gap, as seen in Fig. 1. This means that the inductance does not vary with the magnetic field strength generated by the inductor coils in the operating region. When the core is close to saturation, then there is rapid change in inductance from its initial value to zero as shown in Fig. 1 [1], when μ_r reduces from its initial value to zero.

1.1. Inductors with variable permeability

Powdered iron cores come under the category of distributed air gap cores. They have small air gaps distributed evenly throughout the cores. There a number of powder iron cores that are commercially available – for example Kool Mμ®, MPP, High Flux, XFlux®, AmoFlux® cores from magnetics or powder cores from Micrometals. These cores differ from ferrite cores in a number of ways.

1. The permeability of the core is dependent only on the core material. Powdered iron core thus have a 'fixed' distributed air gap. This is unlike ferrites where the air gap and number of turns can be varied for the same inductance to give the least inductor losses.
2. The powered iron cores have a higher saturation flux density B_{sat} which can be more than twice as that of ferrite cores [2]. 60μ KoolMμ, Epcos N87 ferrite cores have a B_{sat} of 1000mT and 490mT respectively [3]. This means that fewer parallel core sets would be required to build high current inductor in high power density converters [4]–[6].
3. With increase in magnetic field strength, the small pieces of powdered iron gradually saturate one after the other starting with the smallest piece of iron. The process is called soft saturation [7]. This results in the permeability of the core to slowly reduce with increase in inductor current [8], as seen in Fig. 1 and Fig. 2.
4. There is no fringing flux in the air gap, unlike ferrite cores as seen in Fig. 1. This eliminates additional copper losses in the winding at high frequencies.
5. Powdered iron cores have much higher core losses when compared to ferrites, by a factor of ten to fifty times depending on the manufacturer and operating currents [2].

Due to the soft saturation, the permeance of the core depends on the magnetic field strength. With increase in the ampere-turns, the permeance reduces gradually. While this dependency is largely non-linear, the variation can be linearized in the operating region of the inductor, as shown in Fig. 2 for a KoolMμ E65 core of permeability 26μ, 40μ, 60μ and a Micrometal core of permeability 35μ, 60μ and 75μ. The inductance variation can be expressed by (3), where A_{L0} is the permeance at zero ampere-turns and M is the slope of the permeance (or permeability) variation as a function of ampere-turns. As a result, the inductance L linearly varies with inductor current i_L given by (4) where L_0 is the inductance at zero current and K is the slope of inductance reduction with current. K and M can hence be related by a factor of N^3:

$$A_L = A_{L0} - M(Ni_L) \quad (3)$$

$$L = L_0 - Ki_L \quad (4)$$

$$K = N^3 M \quad (5)$$

It is common that manufacturers provide information regarding the variation of permeance with ampere-turns as shown in Fig. 2. Since the inductance continuously varies with current, it has two important effects.

1. The slope of the current varies with time and this causes non-linear currents through the inductor, unlike what is found in ferrites.
2. Secondly, the reduction in inductance necessitates the oversizing of inductance so that there is sufficient inductance L_{min} at the maximum inductor current [8].

2. Estimation of ripple and inductance roll-off of variable permeability cores based on operating conditions

For DC/DC converters especially boost, buck, buck-boost and flyback converters, two modes of operation are possible – continuous conduction mode (CCM) and discontinuous conduction mode (DCM). In both modes, there is a current ripple ΔI_L through the inductor and in case of CCM, there is a continuous average DC current through the inductor $I_{L(avg)}$. Fig. 3 shows the inductor current waveforms for a boost converter where D is the duty cycle [9].

In CCM,

$$I_{L(max)} = I_{L(avg)} + \Delta I_L/2 \quad (6)$$

$$I_{L(min)} = I_{L(avg)} - \Delta I_L/2 \quad (7)$$

In DCM,

$$I_{L(min)} = 0 \qquad I_{L(max)=}\Delta I_L \quad (8)$$

The current ripple Δi_L is dependent on the inductance as shown in (2). However, when using powdered iron cores, the inductance is itself is dependent on the current through it. This interdependency makes it difficult to directly calculate the either the inductance or the ripple, as in (2). This also means that the determination of the inductor cores losses will be inaccurate as the core losses depend on the ripple estimation [2] and the corresponding peak-peak variation in flux density ΔB, as given by the Steinmetz equation

$$P_{core} = A\, f_{sw}^{a} B_{pk}^{b}\, V_e \quad (9)$$

$$B_{pk} = \frac{\Delta B}{2} = \mu_0 \mu_r \frac{\Delta H}{2} = \frac{\mu_0 \mu_r}{2}\left(\frac{N \Delta i_L}{l_e}\right) \quad (10)$$

where V_e is volume of core, A,a,b are the Steinmetz parameters, f_{sw} is the switching frequency and B_{pk} = $\Delta B/2$. (Even though the Steinmetz equation is applicable for sinusoidal inductor currents, in the above situation it is being approximated for DC application). In order to manage

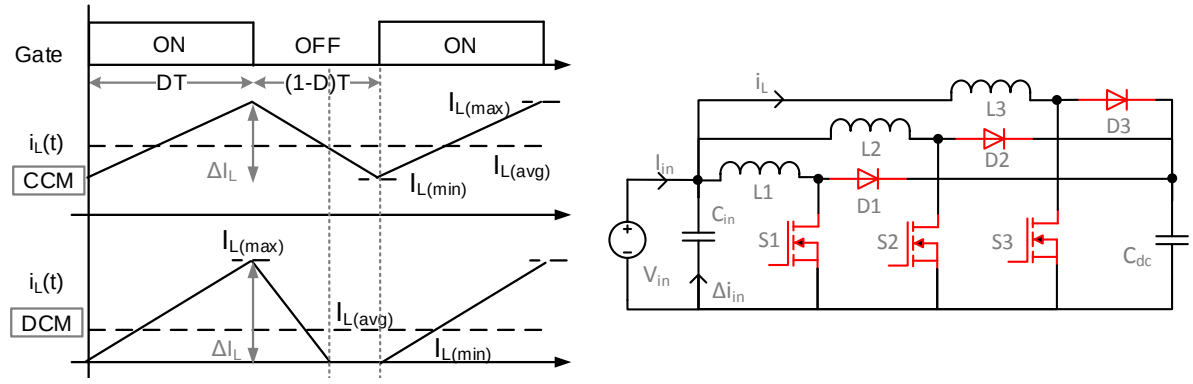

Fig. 3. Inductor current with ripple for a boost converter operating in CCM and DCM modes (left). Topology of interleaved boost converter used for experimental verification (right)

the interdependency between inductance and inductor current when using cores with variable permeability and to determine both the parameters, four approaches can be made:

1. Considering no inductance variation

This case is similar to the case of ferrites. Without considering inductance reduction due to ampere-turn, the inductance will be the estimated by setting *K=0* in (4). The inductance will be the highest at $L=L_0$ and the estimated ripple will be the lowest, as shown in (11) and (12). This method will lead to under-sizing of the inductor with respect to the actual design requirements and underestimation of the inductor ripple and core losses.

$$L = L_0, \qquad K = 0 \tag{11}$$

$$\Delta I_L = \frac{V_L}{L_0}\Delta t \tag{12}$$

2. Using peak current $I_{L(max)}$ to determine the inductance

In this method, the peak inductor current is used to determine the operational inductance. Using (12), the inductor ripple is estimated assuming no inductance variation. Then using equations (6),(7),(8) and based on the mode of operation, the maximum inductor current $I_{L(max)}$ can be determined. The operational inductance and actual ripple can be estimated as:

$$L_{min} = L_0 - KI_{L(max)} \tag{13}$$

$$L_{max} = L_0 - KI_{L(min)} \tag{14}$$

$$\Delta i_L = \frac{V_L}{L_{min}}\Delta t = \frac{V_L}{L_0 - KI_{L(max)}}\Delta t \tag{15}$$

Estimating the ripple based on $I_{L(max)}$ will give the lowest possible value of inductance and overestimation of the ripple and the core losses. In practice, the measured ripple will be lower than that estimated by (15) but higher than that estimated by (12). This is because, as the current increases from $I_{L(min)}$ to $I_{L(max)}$, the inductance will reduce from L_{max} to L_{min}. Estimating the ripple based on $I_{L(max)}$ will hence lead to over-sizing the required size of passive filters and overestimating the core losses.

3. Using middle current $I_{L(mid)}$ to determine the inductance

Based on the above argument, a simple way to consider the inductance variation is to use the inductor middle current, $I_{L(mid)}$. Using (12), the inductor ripple is estimated assuming no inductance variation. Then using equations (6),(7),(8) and based on the mode of operation, the middle inductor current $I_{L(mid)}$ can be determined by (16):

$$I_{L(mid)} = \left(I_{L(max)} + I_{L(min)}\right)/2$$

For CCM,
$$I_{L(mid)} = I_{L(avg)} \tag{16}$$

For DCM,
$$I_{L(mid)} = \Delta I_L/2$$

$$L = L_0 - KI_{L(mid)} \tag{17}$$

$$\Delta i_L = \frac{V_L}{L_{\mathrm{mid}}}\Delta t = \frac{V_L}{L_0 - KI_{L(mid)}}\Delta t \tag{18}$$

The operational value of inductance averaged over a time period and the corresponding inductor ripple can be estimated by (17) and (18) respectively. The accuracy of this method is largely dependent on the mode of operation. In CCM with a small ripple Δi_L in relation to the average current, the approximation can be made that $\Delta i_L/I_{L(avg)} \approx 0$. In such a situation, the inductance is largely determined by the DC bias due to the $I_{L(avg)}$. The inductance and ripple can be estimated based on (17) and (18) with high accuracy. However in DCM or BCM, this approximation will never hold true as $\Delta i_L/I_{L(\mathrm{mid})}$ will differ by a factor of two. In such a situation we need to mathematically solve the ripple, inductance dependence as shown in next section.

4. Differential equation for determination of non-linear inductor current

To get accurate estimation of inductance and ripple when using variable permeability cores, it is essential to mathematically derive the inductance-current dependence. A time dependent variation of inductance can be written based on (4) as

$$L(t) = L_0 - Ki_L(t) \tag{19}$$

$$V_L = L(t)\frac{di_L(t)}{dt} = \left(L_0 - Ki_L(t)\right)\frac{di_L(t)}{dt} \tag{20}$$

The inductor current $i_L(t)$ as a function of time can be expressed as a first order non-linear ordinary differential equation shown above. The solution to this differential equation is

$$V_L t = \left(L_0 i_L(t) - \frac{Ki_L(t)^2}{2}\right) + C_1 \tag{21}$$

Using the initial condition that at *t=0, i_L=$i_{L(0)}$*

$$C_1 = -\left(L_0 i_{L(0)} - \frac{Ki_{L(0)}^2}{2}\right) \tag{22}$$

Using (22) in (21),

$$\frac{Ki_L(t)^2}{2} - L_0 i_L(t) + \left(V_L t + L_0 i_{L(0)} - \frac{Ki_{L(0)}^2}{2}\right) = 0 \tag{23}$$

$$i_L(t) = \frac{L_0}{K} - \sqrt{\frac{L_0^2}{K^2} - \frac{2}{K}\left(V_L t + L_0 i_{L(0)} - \frac{Ki_{L(0)}^2}{2}\right)} \tag{24}$$

(23) is a quadratic equation in $i_{L(t)}$ and it has two roots. When V_L is positive, current through the inductor increases. So of the two solutions, the negative solution is correct and is shown in (24). The above equation can hence be used to determine the non-linear current through an inductor with variable permeability. The equation is applicable not only to powdered iron cores but to all cores that exhibit a linear variation in permeability with DC bias.

3. Ripple and inductance estimation applied to a boost converter

Using a boost converter as an example, the derived mathematical model is applied to both CCM and DCM mode of operation. For DCM, $i_{L(0)}$= *0* as seen in Fig. 3 and (24) can be written as (25) where *t=DT* is the ON time of the switch when inductor current increases. Based on this, the ripple $\Delta i_{L(DCM)}$ and the average inductance $L_{avg(DCM)}$ over a time Δt in DCM can be expressed as in equation (26) and (27) respectively:

$$i_L(t) = \frac{L_0}{K} - \sqrt{\frac{L_0^2}{K^2} - \frac{2V_L t}{K}} \tag{25}$$

$$\Delta i_{L(DCM)} = i_{L(max)} = \frac{L_0}{K} - \sqrt{\frac{L_0^2}{K^2} - \frac{2V_L(DT)}{K}} \tag{26}$$

$$L_{avg(DCM)} = \frac{V_L \Delta t}{\Delta i_L} = \frac{V_L \Delta t}{\left(\frac{L_0}{K} - \sqrt{\frac{L_0^2}{K^2} - \frac{2V_L \Delta t}{K}}\right)} \tag{27}$$

For CCM, with $i_{L(0)} = i_{L(\min)}$ the switch is ON till *t=DT* as seen in Fig. 3. The ripple in CCM $\Delta i_{L(CCM)}$ and average inductance $L_{avg(CCM)}$ over a time Δt can be expressed as:

$$i_L(t) = \frac{L_0}{K} - \sqrt{\frac{L_0^2}{K^2} - \frac{2}{K}\left(V_L t + L_0 i_{L(\min)} - \frac{Ki_{L(\min)}^2}{2}\right)} \tag{28}$$

$$\Delta i_{L(CCM)} = i_{L(\max)} - i_{L(min)} = \left\{ \frac{L_0}{K} - \sqrt{\frac{L_0^2}{K^2} - \frac{2}{K}\left(V_L(DT) + L_0 i_{L(\min)} - \frac{K i_{L(\min)}^2}{2} \right)} \right\} - i_{L(\min)} \quad (29)$$

$$L_{avg(CCM)} = \frac{V_L \Delta t}{\left(\frac{L_0}{K} - \sqrt{\frac{L_0^2}{K^2} - \frac{2}{K}\left(V_L(\Delta t) + L_0 i_{L(\min)} - \frac{K i_{L(\min)}^2}{2} \right)} - i_{L(\min)} \right)} \quad (30)$$

From a practical design perspective, since $L_{avg(CCM)}$ and $L_{avg(DCM)}$ will be lower than L_0, it is important to increase the number of turns of the inductor so as to compensate for the loss of inductance and increase of ripple magnitude.

3.1. Simulation of four models using KoolMμ inductor in a boost converter

The above four methods to determine the inductor ripple and inductance are applied to an E65 KoolMμ powdered iron core inductor. Using a bobbin of *N=42* turns, three inductors are built with KoolMμ core of permeability 60μ, 40μ and 26μ. Table 1 shows the core permeability, permeance A_{L0}, permeance variation slope *M* and calculated inductance at zero current L_0. With V_L= ±700V and Δt=15 μs, the inductor current and inductance as estimated by the four methods using MATLAB are shown in Fig. 4 for 60μ core and $i_{L(0)}$=*0* and 30A respectively. The following observations can be made:

- The first two methods assume a constant inductance as a function of time and do not accurately estimate the inductor current. At *t=15μs*, the current estimated by the first and second methods show a difference of more than 10A, as seen in Fig. 4.
- The third method based on the middle current is very good in approximately estimating the inductor current even though it assumes a fixed average inductance. At *t=15μs*, the estimated current deviates from that shown by the fourth method by about 1A.
- The fourth method based on the partial differential equation shows a varying inductance as a function of time and estimates a non-linear current. Method 1 and 2 have error of up to 20% compared to 4. Experimental verification presented in the next section proves that this method is most accurate.

4. Experimental verification using KoolMμ core in boost converter

To verify the proposed model for estimating the ripple, a 10kW three leg interleaved boost converter with powdered iron core inductors and MOSFETs is used [6], as shown in Fig. 3 and Fig. 5. It has a switching frequency of f_{sw}=47kHz and an input voltage range of 350V-700V.

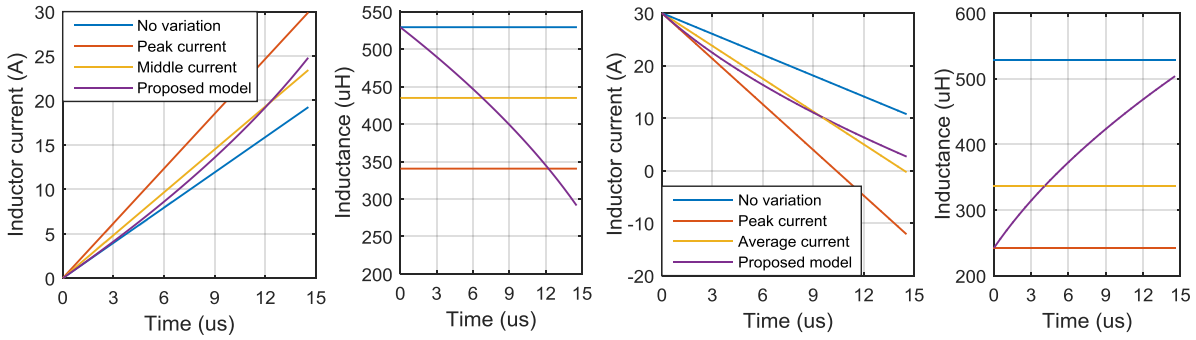

Fig. 4. Inductor current and inductance estimated by four methods for L_0=529.2μH using 60μ KoolMμ core with (left) V_L=700V, Δt=15 μs, i_{L0}=0 and (right) V_L= -700V, Δt=15μs, i_{L0}=30A;

μr	A_{L0} (nH)	M (nH/A)	N	K (nH/A)	L_0 (μH)	$L_{@10A}$ (μH)	$L_{@10A}$ (%)
60μ	300	181/1400	42	9.58	529	433.21	81.89
40μ	230	143/2200	42	4.82	405	356.84	88.11
26μ	162	106/3500	42	2.24	285	262.56	92.13

Table 1 – KoolMμ core inductors with their corresponding permeance and inductance

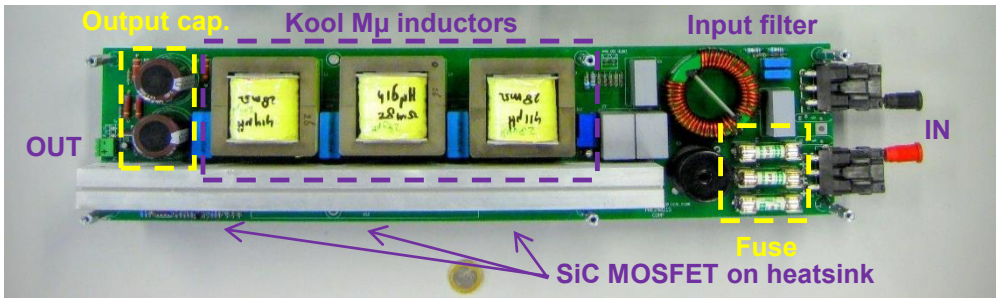

Fig. 5. Practical setup of interleaved boost converter with three KoolMμ 26μ E65 cores

It is operated at a fixed output voltage of V_{out}=750V. The maximum current through the inductors L1, L2, L3 is $I_{L(avg)}$=10A and it occurs when the input is P_{in}=10kW, V_{in}=350V, I_{in}=30A and the input current I_{in} is shared between the three legs. Table 1 shows the actual and percentage inductance $L_{@10A}$ at 10A. It can be seen that the operational inductance is reduced by 8% to 18% depending on the core permeability.

Experimental measurements of the inductor ripple from the boost converter using the 26μ core with L_0=284μH are shown in Table 2 and Fig. 6. The measurements are compared with estimation of inductor ripple from the four proposed methods in the table. Error of up to 5% is obtained if method 1 and 2 are used for ripple estimation. Method 3 and 4 are close to experimental measurements with less than 0.05% error, showing a ten times reduction in error. The estimates from Method 3 and 4 are very close in value in this case, that it can be concluded that method 3 is an excellent choice for simplified calculations. In situations where high level of accuracy is required in ripple and current estimation, method 4 can be implemented.

V_L(V)	$I_{L(avg)}$ (A)	Duty (%)	Mode	V_{out} (V)	Inductor ripple (A)				
					Method 1	Method 2	Method 3	Method 4	Meas.
350	2.67	30.5	DCM	750	7.94	8.47	8.20	8.21	8.16
400	4.67	38.5	DCM	750	11.46	12.6	12.00	12.03	12.0
500	3.67	22.6	DCM	750	8.41	9.00	8.70	8.71	8.75
500	1.83	17.8	DCM	750	6.62	6.99	6.80	6.80	6.81
600	3.07	15.2	DCM	750	6.79	7.17	6.97	6.98	6.97

Table 2 – Estimated and experimentally measured value of inductor ripple using 26μ KoolMμ

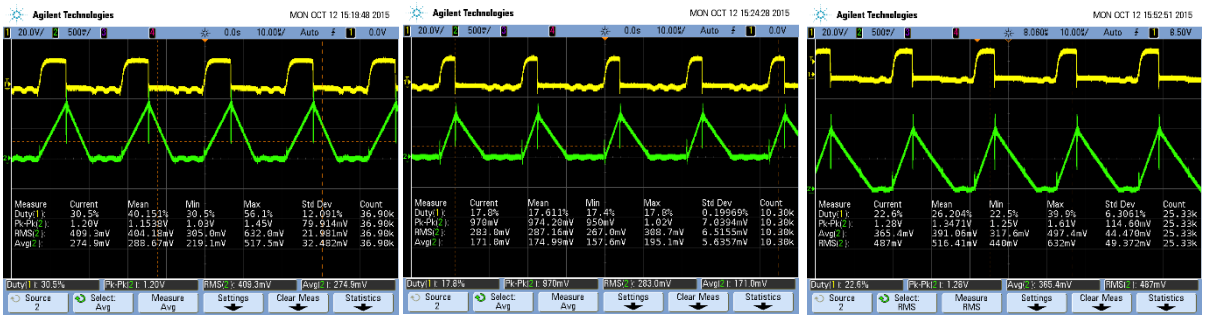

Fig. 6. Gate voltage of the MOSFET and current waveforms of the KoolMμ inductor measured using current probe - V_{in}=350V, $I_{L(avg)}$=8A (left); V_{in} =500V, I_{in} =5.5A (middle); V_{in} =500V, I_{in} =11A (right);

5. Conclusion

Powdered iron core inductors are excellent choice for use in high power density converters due to their high saturation flux density. The core exhibits a gradual saturation and reduction of inductance with increasing ampere-turns, unlike ferrites that abruptly reduce to zero inductance near the saturation region. As a result of soft saturation, the inductance varies as function of inductor current resulting in non-linear currents. This paper provides a mathematical derivation of this non-linear behavior for both continuous and discontinuous mode of converter operation. The non-linear model is compared with three other simplified approaches, of which the middle-current method gives the closest results. Experimental verification using KoolMμ powered iron core in a boost converter have proven the accuracy of the proposed model.

Acknowledgements

The authors would like to thank the guidance and support of PhD student V. Prasanth from Delft University of Technology; Power Research Electronics B.V, Breda especially to M.Kardolus and M.v.d. Heuvel; and ABB EV Charging Infrastructure, Rijswijk. The research was sponsored by TKI switch2smart grids grant Netherlands.

References

[1] MAGNETICS, “Technical Bulletin MAGNETICS KOOL Mμ® E-CORES,” 2005.
[2] M. S. Rylko, K. J. Hartnett, J. G. Hayes, and M. G. Egan, “Magnetic Material Selection for High Power High Frequency Inductors in DC-DC Converters,” in *IEEE Applied Power Electronics Conference and Exposition*, 2009, pp. 2043–2049.
[3] “Ferrites and accessories - SIFERRIT material N87,” Epcos, pp. 1–7, 2006.
[4] G. R. Chandra Mouli, P. Bauer, M. Zeman, G. R. C. Mouli, P. Bauer, and M. Zeman, “Comparison of system architecture and converter topology for a solar powered electric vehicle charging station,” in *2015 9th International Conference on Power Electronics and ECCE Asia (ICPE-ECCE Asia)*, 2015, pp. 1908–1915.
[5] G. R. Chandra Mouli, P. Bauer, and M. Zeman, “System design for a solar powered electric vehicle charging station for workplaces,” *Applied Energy*, vol. 168, pp. 434–443, Apr. 2016.
[6] G. Ram, Chandra Mouli, Jos, Schijffelen, Pavol, Bauer, and M. Zeman, “Design and Comparison of a 10kW Interleaved Boost Converter for PV Application Using Si and SiC Devices,” *IEEE J. Emerg. Sel. Top. Power Electron. under Rev.*, 2016.
[7] Bong-Gi You, Jong-Soo Kim, Byoung-kuk Lee, Gwang-Bo Choi, Dong-Wook Yoo, B.-G. You, J.-S. Kim, B. Lee, G.-B. Choi, and D.-W. Yoo, “Optimization of powder core inductors of buck-boost converters for Hybrid Electric Vehicles,” in *2009 IEEE Vehicle Power and Propulsion Conference*, 2009, pp. 730–735.
[8] J. D. Pollock, W. Lundquist, and C. R. Sullivan, “Predicting inductance roll-off with dc excitations,” in *IEEE Energy Conversion Congress and Exposition*, 2011, pp. 2139–2145.
[9] N. Mohan and T. Undeland, “Power electronics: converters, applications, and design,” 2007.